Optical Engineering

SPIEDigitalLibrary.org/oe

Broadband optical cosite interference cancellation

Jonathan Bruno
Maddie Lu
Yanhua Deng
Paul Prucnal

Broadband optical cosite interference cancellation

Jonathan Bruno
Naval Research Laboratory
Washington, DC 20375
E-mail: jonathan.bruno@nrl.navy.mil

Maddie Lu
Yanhua Deng
Paul Prucnal
Princeton University
Department of Electrical Engineering
Princeton, New Jersey 08544

Abstract. Here, we provide an overview of broadband cosite interference reduction using an optical system to perform incoherent counter-phase modulation and subtraction. The equation governing interference cancellation depth is derived and discussed with respect to two key parameters, attenuation and delay accuracy. Cancellation depth is then examined with respect to signal bandwidth and device parameters to provide a context for predicted cancellation performance. Experimentally recorded interference cancellation data is presented along with predicted performance to show the agreement of theory and data. [DOI: 10.1117/1.OE.52.5.053001]

Subject terms: microwave photonics; radio over fiber; radio frequency photonics; cosite interference; counter-phase modulation.

Paper 121907 received Jan. 7, 2013; revised manuscript received Mar. 25, 2013; accepted for publication Apr. 4, 2013; published online May 7, 2013.

1 Introduction

Photonic devices are fundamentally attractive for applications involving data transmission in the radio-frequency (RF) spectrum. The inherent features of photonic links, such as resistance to electromagnetic interference, low-loss fiber transmission, high precision tuning, and large instantaneous bandwidth in the RF spectrum, offer unique advantages compared with traditional RF electronics.[1] Radio-over-fiber systems have been implemented in applications such as wireless communications, optical beam forming, arbitrary waveform generation, long-haul antenna remoting, and recently cosite interference reduction.[2–6]

Cosite interference can be defined as the unintentional reduction of a receivers signal-to-noise ratio resulting from a colocated transmitter. Receiver degradation through local interference is a common problem on cell phone towers, mobile platforms, and communications base stations.[7–9] With the proliferation of modern wireless communications, cosite interference is increasingly problematic and will only worsen over time.[9] There are a large number of existing interference cancellation techniques for digital and analog signals such as filtering, multiuser detection, and beamforming.[8–10] While all of these techniques posses individual merits, research suggests that the combination of techniques and technologies should provide the most robust interference cancellation solutions.[10] In particular, optical techniques for reducing interference cancellation are complementary to many traditional interference reduction techniques while offering high linearity and large operational bandwidth. Microwave photonics techniques for interference reduction are an active area of research as these systems do not suffer the bandwidth or linearity limitations of electronic techniques; current research looks to provide significant improvements to both cancellation depth and bandwidth.[11,12]

The proof-of-concept optical cancellation system (OCS) represents a radio-over-fiber system that reduces cosite interference based on the technique of incoherent counter-phase modulation. The OCS has demonstrated over 80 dB/Hz and 45 dB/Hz of interference signal rejection for single tone and broadband (100 MHz) interference, respectively.[13] The purpose of this paper is to examine the theoretical and practical limits of cancellation performance as they relate to optical attenuation and delay accuracy. Explicitly describing interference cancellation in terms of device parameters enables a practical method of predicting system performance based on component selection. This is important as it not only expands the previous systems characterization and provides a context for previously reported results,[6,13] but also describes a rationale for system construction based on specific application requirements. Section 2 describes the system architecture while Sec. 3 derives an expression for cancellation depth based on signal attenuation and delay. The mathematical description is included to provide a robust explanation of system performance. Section 4 expands the description of cancellation depth to include frequency dependent channel response and discusses modulator frequency response mismatch. Section 5 discusses broadband cancellation performance and presents a comparison of measured and predicted interference signal reduction.

2 System Architecture Overview

The optical cancellation system is a three-port system consisting of two input RF channels and an output RF channel. The input channels are true-time delay matched and represent the noisy receiver signal and reference interference signal routed from the receive and transmit antennas. Each RF signal is sent to a quadrature biased electro-optic modulator that amplitude modulates the RF signal onto an optical carrier. Using the method of counter phase modulation, where the two modulators are biased on opposite transmission slopes (i.e., positive and negative), a π phase difference is introduced between the two signals. The channel carrying the reference interference signal is processed in the optical domain with variable attenuation and delay to match the amplitude and phase characteristics of the noisy receiver signal. Ideally, with highly accurate channel matching, the amplitude and phase of the interference signal should be near identical in both channels, except for the phase inversion between the modulators. Combining the two signals added in a 50:50 optical coupler, the resulting signal is

0091-3286/2013/$25.00

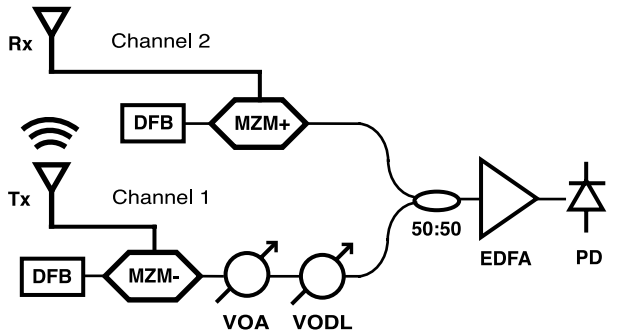

Fig. 1 Optical cancellation system architecture. Channel 1 carries the interference signal to the negative quadrature biased modulator, variable optical attenuator, and variable optical delay line. Channel 2 refers to the receive antenna output, which is coupled to the positive quadrature biased modulator. The two channels are then combined in a 50:50 optical coupler and amplified prior to the photodetector.

then amplified by an erbium doped fiber optical amplifier and converted back to an electrical signal through a high responsivity photodetector. A system diagram of the OCS is found in Fig. 1, for a more detailed account of the system architecture please refer to Suarez.[6]

3 Cancellation Performance

To derive an expression for cancellation performance we first describe the RF input signals. The reference signal tapped directly from the RF transmitter can be represented as $S_0(t) = V_0 \sin(\Omega t)$, where V_0 represents the amplitude voltage and Ω is the angular frequency of the RF signal. The signal transmitted through free-space and incident on the receive antenna can be represented by $S_1(t) = \gamma S_0(t-\tau)$, where γ and τ represent attenuation and delay. The reference signal $S_0(t)$ enters the OCS through channel 1, while the transmitted signal $S_1(t)$ enters through channel 2. The modulation signals for channels 1 and 2 can be described by

$$\phi_1(t) = \phi_{\mathrm{dc}}^- + \phi_{\mathrm{rf}} \sin(\Omega t) \tag{1}$$

$$\phi_2(t-\tau) = \phi_{\mathrm{dc}}^+ + \gamma\phi_{\mathrm{rf}} \sin[\Omega(t-\tau)], \tag{2}$$

where the term $\phi_{rf} = \pi V_0/V_\pi(\Omega)$ represents the amplitude of the modulated signal in terms of the device parameter V_π.[14] The terms ϕ_{dc}^+ and ϕ_{dc}^- represent positive and negative quadrature bias, which can be understood as $\phi_{\mathrm{dc}}^+ = \pi(2n + 1/2)$ and $\phi_{\mathrm{dc}}^- = \pi[(2n+1) + 1/2]$.

After entering the OCS, the reference channel is attenuated and delayed to match the channel carrying the transmitted signal. The channels are then combined and amplified before arriving at the photodetector. The electric field of the optical signal at the photodetector can be expressed as

$$E_{\mathrm{opt}} = \zeta\left[e^{i\varphi} \sin\frac{\phi_1(t-\tau)}{2} + \sqrt{\beta}e^{i\varphi'} \sin\frac{\phi_2(t-\tau')}{2}\right], \tag{3}$$

where $\varphi = \omega_1 t$ and $\varphi' = \omega_2(t-\tau')$ represent the phase of the two optical carriers, set such that $\omega_1 \neq \omega_2$. The terms β and τ' represent the user defined power attenuation and delay, and $\zeta = iE_{\mathrm{in}}\sqrt{G_0\alpha}$ represents the field strength, where the terms G_o and α represent net optical gain and the optical power loss factor of the modulator, respectively. The expression also assumes equal optical power in both channels expressed as $E_{\mathrm{in}}(t) = \kappa\sqrt{2P_{\mathrm{laser}}}$, where P_{laser} is the average laser power and the term κ is a constant relating field and average power such that $P_{\mathrm{laser}} = E_{\mathrm{in}}^* E_{\mathrm{in}}/(2\kappa^2)$.[3] With the expression for total electric field the average optical power can be expressed as

$$P_{\mathrm{opt}} = z\left\{\sin^2\left(\frac{\phi_1}{2}\right) + \beta\sin^2\left(\frac{\phi_2}{2}\right) + 2\sqrt{\beta}\cos(\Delta\varphi)\sin\left(\frac{\phi_1}{2}\right)\sin\left(\frac{\phi_2}{2}\right)\right\}. \tag{4}$$

Here $z = P_{\mathrm{laser}}G_0\alpha$ and $\Delta\varphi = (\omega_1 t - \omega_2 t + \omega_2\tau')$ represents the beat frequency of the two optical carriers. The OCS system is designed to push the beat frequency beyond the bandwidth of the photodetector.[6] The threshold for meeting this requirement can be determined by examining how the mixing between the optical beat frequency and the modulated RF frequency compare to the detector bandwidth. In order to determine this threshold it is necessary to find the lowest frequency term with a dependence on $\Delta\varphi$, which is accomplished by expanding the expression for optical power [Eq. (4)] with respect to the beat frequency terms. Here, we have substituted Eqs. (1) and (2) into Eq. (4):

$$P_{\mathrm{opt}}(\Delta\varphi) = 2z\sqrt{\beta}\cos(\Delta\varphi)\cos\left\{\frac{\phi_{\mathrm{dc}}^+ - \phi_{\mathrm{dc}}^-}{2} + \frac{\phi_{\mathrm{rf}}}{2}[\gamma\cos(\Omega\tau) - \cos(\Omega\tau')]\sin(\Omega t) + \frac{\phi_{\mathrm{rf}}}{2}[\sin(\Omega\tau) - \gamma\sin(\Omega\tau')]\cos(\Omega t)\right\}, \tag{5}$$

This equation describes a periodic function of two periodic functions, which can be expanded to produce a series of modulated Bessel functions. The optical beat frequency is multiplied by the modulated Bessel functions and therefore produce sum and difference frequency sidebands.[15] It is important to consider both the sideband frequencies as well as the optical beat frequency relative to photodetector bandwidth to ensure that any potential intermodulation products are outside the detector bandwidth. Expanding Eq. (5) with the Jacobi-Anger identity[16] shows that the lowest order sum and difference sidebands are described by $\cos(4n\Omega t \pm \Delta\varphi)$. The condition for pushing the optical beat frequency beyond the detector bandwidth is then related to the wavelength of the two carrier signals, λ_1 and λ_2, and described by the expression

$$4nf_{\mathrm{rf}} - c\left(\frac{1}{\lambda_1} - \frac{1}{\lambda_2}\right) > B, \tag{6}$$

where $n = 1, 2, 3, \ldots, c$ is the speed of light, f_{rf} is the RF signal frequency, and B is the photodetector bandwidth.

Once we have ensured that the condition for filtering the optical beat frequency with the photodetector is met, we can ignore the beat frequency terms in the average optical power and proceed to calculate the photocurrent in the detector. Using the expression $i_{\mathrm{pd}} = \Re P_{\mathrm{opt}}$ where $\Re$ is the detector responsivity, we arrive at the following equation for photocurrent,

$$
\begin{aligned}
i_{\mathrm{pd}} = i_{\mathrm{dc}}\{1+\beta-\cos(\phi_{\mathrm{dc}}^{+})J_0(\gamma\phi_{\mathrm{rf}})-\beta\cos(\phi_{\mathrm{dc}}^{-})J_0(\phi_{\mathrm{rf}})\} \\
-2i_{\mathrm{dc}}\cos(\phi_{\mathrm{dc}}^{+})\sum_m J_m(\gamma\phi_{\mathrm{rf}})\cos[m\Omega(t-\tau)] \\
+2i_{\mathrm{dc}}\beta\cos(\phi_{\mathrm{dc}}^{-})\sum_m J_m(\phi_{\mathrm{rf}})\cos[m\Omega(t-\tau')] \\
+2i_{\mathrm{dc}}\sin(\phi_{\mathrm{dc}}^{+})\sum_k J_k(\gamma\phi_{\mathrm{rf}})\sin[k\Omega(t-\tau)] \\
-2i_{\mathrm{dc}}\beta\sin(\phi_{\mathrm{dc}}^{-})\sum_k J_k(\phi_{\mathrm{rf}})\sin[k\Omega(t-\tau')],
\end{aligned}
\tag{7}
$$

this expression for photocurrent distinguishes even, odd, and dc-terms based on the order of the Bessel function, where $n = 0, 1, 2, 3\ldots$ and $m = 2n$ represent even terms and $k = 2n+1$ represent odd terms. The dc current is defined as $i_{\mathrm{dc}} = \Re P_{\mathrm{laser}} G_0 \alpha_{\mathrm{MZM}}/2$.

We can provide a more intuitive representation of output photocurrent by incorporating the Bessel function multiplication theorem which states, $J_\nu(\gamma\phi_{\mathrm{rf}}) \approx \gamma^\nu J_\nu(\phi_{\mathrm{rf}})$ in the small signal limit where $(|\gamma^2-1|) > 1$ and J_ν is approximately constant.[16] Comparing the simplified expression $\gamma^\nu J_\nu(\phi_{\mathrm{rf}})$ to the user defined attenuation β we quickly see that this technique cannot compensate for harmonics that occur when $\nu > 1$, thus cancellation performance is limited to the fundamental signal. By setting each modulator to positive and negative quadrature bias, such that $\phi_{\mathrm{dc}}^{+} = \pi/2$ and $\phi_{\mathrm{dc}}^{-} = 3\pi/2$, we can remove the effects of the even harmonics. Thus, the counter-phase modulation technique produces a third order limited system. The expression for output photocurrent at the fundamental frequency is described by

$$
\begin{aligned}
i_{\mathrm{pd}} = i_{\mathrm{dc}}(1+\beta) + 2i_{\mathrm{dc}}J_1(\phi_{\mathrm{rf}}) \\
\times\{[\gamma\cos(\Omega\tau)-\beta\cos(\Omega\tau')]\sin(\Omega t) \\
+[\gamma\sin(\Omega\tau)-\beta\sin(\Omega\tau')]\cos(\Omega t)\}.
\end{aligned}
\tag{8}
$$

The average RF output power can then be found by using the familiar expression $P = i_{\mathrm{pd}}^2 R/2$ where R is the resistance of the photodiode; note that this expression does not account for impedance matching where maximum power transfer requires an adjustment of −6 dB.[3] The expression for power can be simplified by defining $\tau' = \tau - \Delta\tau$, where $\Delta\tau$ represents the deviation from perfect channel delay matching. Defining the terms $P_{\mathrm{dc}} = i_{\mathrm{dc}}^2(1+\beta)^2 R/2$ and $P_0 = 2i_{\mathrm{dc}}^2 J_1^2(\phi_{\mathrm{rf}})R$ we have an expression for the output power

$$
P = P_{\mathrm{dc}} + P_0\{\gamma^2+\beta^2-2\gamma\beta\cos(\Omega\Delta\tau)\}\cos(\Omega t). \tag{9}
$$

This expression shows that as β approaches γ and $\Delta\tau$ approaches zero, the output power of the RF signal approaches zero. While a description of the output RF signal power is instructive, we are interested in the expected RF signal reduction with respect to the accuracy of the channel delay and amplitude matching. Therefore, we define β as the user defined attenuation plus the device amplitude precision such that $\beta = (\gamma + \Delta\gamma)$, then take the ratio of the RF signal strength for the system output and the transmitted signal, i.e., $P_{\mathrm{rf}}(S_0+S_1)/P_{\mathrm{rf}}(S_1)$. In a practical sense this is the equivalent to comparing the system output with both channels with the system output without the reference channel. Mathematically the expression for $P_{\mathrm{rf}}(S_1)$ can be found by setting $\beta = 0$. We then represent the reduction in interference signal power at the fundamental frequency $\Omega/2\pi$ by the expression

$$
P_{\mathrm{tx}} = \left(\frac{\Delta\gamma}{\gamma}\right)^2 + 2\left(1+\frac{\Delta\gamma}{\gamma}\right)[1-\cos(\Omega\Delta\tau)]. \tag{10}
$$

This is a convenient description of system performance since it directly equates channel matching precision with cancellation depth. It is important to note that for the special cases where $\gamma = \beta$ and $\tau = \tau'$ Eqs. (9) and (10) resemble the expressions for cancellation performance reported by Suarez.[13] Furthermore, this expression directly relates to the experimental method by which we typically measure cancellation performance, allowing the direct comparison of measured and calculated cancellation depth. Figure 2 shows the calculated cancellation depth for a variety of attenuation and delay accuracy values referenced to 1 GHz. The plot provides a useful point of reference for determining the dominant parameter limiting cancellation performance. For practical purposes, the resolution of the optical delay accuracy is sufficiently high such that, without the influence of other factors, low frequency performance is set by the attenuation accuracy.

4 Frequency Response Mismatch

4.1 *Broadband Cancellation Performance*

Thus far the discussion of cancellation depth has been limited to the case, where channel mismatch solely represents device precision. While device precision limited performance is useful for predicting narrowband signal cancellation, it is important to account for frequency dependent channel mismatch when considering broadband cancellation. While channel mismatch can be the result of a variety of factors, we limit our discussion to channel mismatch directly resulting from components of the OCS. Since the response of the detector is common to both channels the electro-optic modulators act as the dominant source for mismatch. The difference in complex frequency response between channels is used to describe the channel mismatch in amplitude and phase. The difference in magnitude is described by the ratio

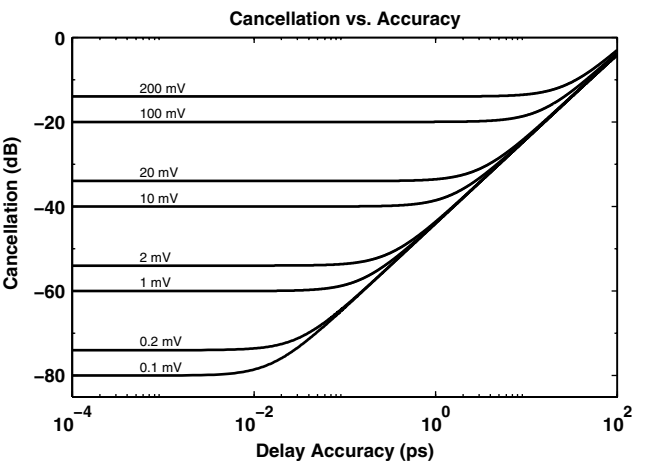

Fig. 2 Calculated cancellation of a 1 GHz signal with varying attenuation and delay device accuracy according to Eq. (10). The values for attenuation accuracy $\Delta\gamma$ are labeled with their associated plots and correspond to values ranging from 0.1 to 200 mV.

of positive and negative modulator device parameters V_{π_1}/V_{π_2} while the difference in phase is described by $\delta\theta = \theta_2 - \theta_1$. The modulated RF signal amplitude can then be expressed as

$$\phi_{\mathrm{rf}_1} = \frac{\pi V_o}{V_{\pi_1}(\Omega)} \quad \text{and} \quad \phi_{\mathrm{rf}_2} = \chi(\Omega)\phi_{\mathrm{rf}_1},$$

where the scaling factor $\chi(\Omega) = V_{\pi_1}(\Omega)/V_{\pi_2}(\Omega)$ describes the contribution from the frequency mismatch.

In order to include frequency dependence in the previously derived expressions for photocurrent [Eq. (8)] and output RF power [Eq. (9)] we redefine the term $\beta + \Delta\gamma$ to include channel attenuation mismatch as $\chi\beta + \Delta\gamma$. Similarly, we can include phase mismatch between the channels by redefining $\tau' = \tau - \Delta\tau - \delta\theta/\Omega$. It is important to note that the frequency dependent mismatch does not effect device accuracy $\Delta\gamma$ or $\Delta\tau$. The expression for broadband cancellation with frequency dependent mismatch is then described as the ratio of RF output signal power to transmitted signal power, expressed as

$$P_{\mathrm{tx}} = 1 + \left(\frac{\chi\beta + \Delta\gamma}{\gamma}\right)^2 - 2\left(\frac{\chi\beta + \Delta\gamma}{\gamma}\right)\cos(\Omega\Delta\tau + \delta\theta). \tag{11}$$

In the special case when χ can be treated as a constant, due to negligible change in mismatch over a given bandwidth, the user defined attenuation can be set such that $\chi\beta = \gamma$ and Eq. (11) reduces to the expression given by Eq. (10). When frequency mismatch cannot be treated as a constant offset and device accuracy is sufficiently small, such that $\chi\beta \gg \Delta\gamma$ and $\delta\theta \gg \Omega\Delta\tau$, the cancellation depth is set by the difference in channel response.

4.2 *Measured Frequency Response Mismatch*

To find the expected broadband performance of the OCS, we measured the complex frequency response of the channels (S21 scattering parameter) for each channel. The complex response describes the frequency dependent gain and phase of a two-port system across a defined bandwidth. The measured S21 data for each channel is displayed in Fig. 3. In the small signal limit $G_{\mathrm{rf}} \propto 1/V_\pi^2$, thus the magnitude of the complex response can be used to calculate the scaling factor χ, while the phase mismatch $\delta\theta$ is determined by taking the difference of the two channels.

The shape and deviation of the mismatch terms have important implications for broadband signal cancellation. The shape of the difference in response curves will determine how well the user defined delay and attenuation can compensate for channel mismatch. Broadband cancellation will be the most successful for over spectral regions, where the derivative of the response mismatch with respect to frequency is approximately zero. Therefore, considering the measured channel response of the OCS system in Fig. 3, broadband cancellation is most difficult in the spectral region between 20 and 1000 MHz. Although an examination of channel mismatch curvature is useful for understanding general OCS performance over ultra-broadband bandwidths, the standard deviation of channel must also be considered when determining cancellation performance. A large standard deviation can be considered in the same terms as device accuracy. The fluctuation of frequency dependent mismatch terms about a mean value simply do not allow for precise channel matching.

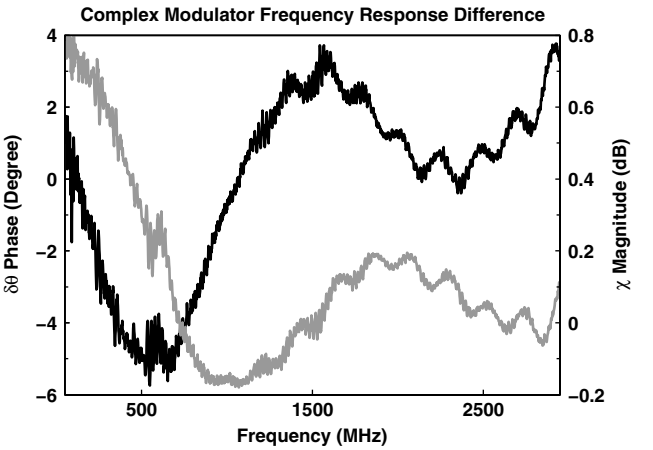

Fig. 3 Measured difference in complex frequency response for the transmit and receive channel modulators. (Black) represents phase mismatch $\delta\theta$, labeled on the *y*-axis left in degrees. (Gray) represents magnitude mismatch χ, labeled on the *y*-axis right in dB.

5 Measured and Predicted Results

A major advantage of working in the optical domain is the availability of high-precision attenuation and delay devices. For example, commercially, attenuators are capable of providing attenuation resolution of. 001 dB with. 1 dB accuracy, which translates to $\Delta\gamma = 0.2$ mV. Furthermore, motorized variable optical delay lines are able provide incremental resolution of ± 40 μm, which translates to $\Delta\tau = 0.1$ ps. It should also be noted that our prototype system employs a manually adjustable delay line, capable of providing fine resolution on the order of 5 μm, which corresponds to $\Delta\tau \approx$ 0.1 ps at the expense of rapid and repeatable tuning.

The OCS takes advantage of these high resolution devices, allowing narrowband cancellation to approach the zero mismatch limit. Unlike narrowband cancellation broadband performance is severely impacted by difference in complex frequency response of the transmit and receive channels. The magnitude and phase mismatch χ and $\delta\theta$ described by Fig. 3 have an overall range of 1 dB and 9.5 deg, respectively. The amplitude and phase mismatch is significantly larger than the device accuracy and will act as the limit for signal cancellation over nearly the entire frequency range.

To show the effect of mismatch on cancellation performance we present Fig. 4, which compares signal rejection with and without frequency mismatch according to Eqs. (10) and (11). The calculated cancellation results are compared directly against measured data. The measured data was recorded with the user defined OCS settings optimized to cancel a narrow bandwidth signal at 1450 MHz. The measured data was recorded over the 50 to 2950 MHz frequency range. Both the measured and predicted results show a minimum signal rejection of 14 dB and mean cancellation of 28 dB for $f_{\mathrm{rf}} > 1$ GHz. In the 200 MHz bandwidth centered around 1450 MHz the mean signal rejection averaged in linear space is 41 dB with peak values >60 dB. The performance improvement is the result of relatively small mismatch values over the bandwidth, where the average values for $\chi\beta/\gamma = .003$ dB and $\delta\theta = 1.4$-deg. For the two

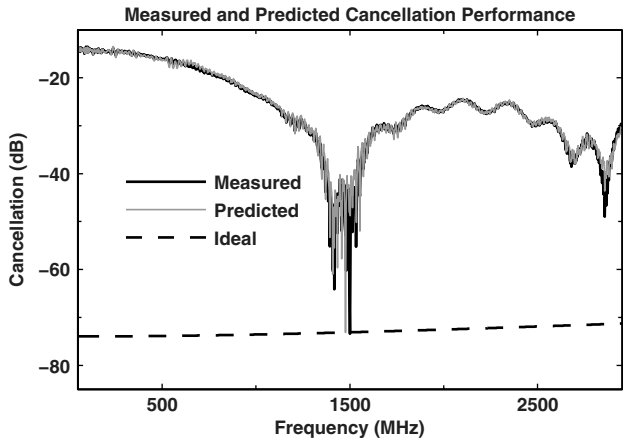

Fig. 4 Measured broadband cancellation compared with simulated cancellation performance, with values for attenuation and delay precision of $\Delta\gamma = 0.2$ mV and $\Delta\tau = 0.01$ ps. Predicted cancellation is based on Eq. (11) and incorporates the measured difference in complex modulator frequency response to produce values for χ and $\delta\theta$. Ideal cancellation corresponds to precision limited performance where $\chi = 0$ dB and $\delta\theta = 0$.

frequencies where cancellation is greatest the measured and predicted results approach the precision-limited case where $\chi\beta = \gamma$ and $\delta\theta = 0$. The values $\Delta\gamma/\gamma = -80$ dB and $\Delta\tau =$ .01 ps were used to calculate the zero mismatch curve are informed by previous measurements of single frequency cancellation performance.[13] The close agreement between the measured data and predicted performance implies that Eq. (11) provides an accurate description of broadband signal rejection using an optical system to perform incoherent counter-phase modulation and subtraction.

6 Conclusion

We have demonstrated the agreement of measured and predicted performance to support the derived expression for broadband interference signal cancellation. We have also shown that cancellation performance is dependent on the fidelity of attenuation and delay matching across the transmit and receive channels. In the case of broadband interference cancellation channel matching is limited by differences in the complex response of the channels rather than device precision. We have demonstrated an average signal rejection 41 dB with peak values >60 dB over a 200 MHz bandwidth, however by improving the pairing of electro-optic modulators the incoherent counter phase-modulation can provide greatly improved signal rejection with increased bandwidth.

Acknowledgments

The authors would like to thank Jason D. McKinney for helpful discussions. This work is supported by STTR Grant #339-6463.

References

1. A. Seeds and K. Williams, "Microwave photonics," *J. Lightwave Technol.* **24**(12), 4628–4641 (2006).
2. J. Capmany and D. Novak, "Microwave photonics combines two worlds," *Nat. Photon.* **1**(6), 319–330 (2007).
3. V. J. Urick et al., "Long-haul analog photonics," *J. Lightwave Technol.* **29**(8), 1182–1205 (2011).
4. I. Lin, J. D. McKinney, and A. Weiner, "Photonic synthesis of broadband microwave arbitrary waveforms applicable to ultra-wideband communication," *IEEE Microw. Wireless Compon. Lett.* **15**(4), 226–228 (2005).
5. J. R. Bruno and P. Prucnal, "Electro-optic cosite interference mitigation," *Proc. SPIE* **7607**, 76071A (2010).
6. J. Suarez, K. Kravtsov, and P. Prucnal, "Incoherent method of optical interference cancellation for radio-frequency communications," *IEEE J. Quant. Electron.* **45**(4), 402–408 (2009).
7. D. Fiedler, "Cosite interference: force XXI communications roadblock," *Army Commun.* **21**(4), 54–59 (1996).
8. K. Allsebrook and C. Ribble, "VHF cosite interference challenges and solutions for the United States Marine Corps' expeditionary fighting vehicle program," in *Military Communications Conference*, Vol. 1, pp. 548–554 (2004).
9. J. Andrews, "Interference cancellation for cellular systems: a contemporary overview," *IEEE Wireless Commun.* **12**(2), 19–29 (2005).
10. G. Boudreau et al., "Interference coordination and cancellation for 4G networks," *IEEE Commun. Mag.* **47**(4), 74–81 (2009).
11. M. Lu et al., "Co-site interference mitigation using optical signal processing," *Proc. SPIE* **8397**, 839705 (2012).
12. J. Suarez and P. Prucnal, "Instantaneous bandwidth of counter-phase optical interference cancellation for RF communications," *IEEE Microw. Wireless Compon. Lett.* **21**(9), 507–509 (2011).
13. J. Suarez and P. Prucnal, "System-level performance and characterization of counter-phase optical interference cancellation," *J. Lightwave Technol.* **28**(12), 1821–1831 (2010).
14. G. Li and P. Yu, "Optical intensity modulators for digital and analog applications," *J. Lightwave Technol.* **21**(9), 2010–2030 (2003).
15. G. N. Watson, *A Treatise on the Theory of Bessel Functions*, Cambridge University Press, Cambridge (1995).
16. M. Abramowitz and I. A. Stegun, *Handbook of Mathematical Functions With Formulas, Graphs, and Mathematical Tables*, Dover Pubns, New York (1964).

Biographies and photographs of the authors are not available.